

CONFIDENTIAL

Copy  
RM L50C14

5

NACA RM L50C14

NACA

# RESEARCH MEMORANDUM

FLIGHT MEASUREMENTS WITH THE DOUGLAS D-558-II

(BuAero No. 37974) RESEARCH AIRPLANE

STATIC LATERAL AND DIRECTIONAL STABILITY CHARACTERISTICS  
AS MEASURED IN SIDESLIPS AT MACH NUMBERS UP TO 0.87

By S. A. Sjöberg

Langley Aeronautical Laboratory  
Langley Air Force Base, Va.

## CLASSIFIED DOCUMENT

This document contains classified information affecting the National Defense of the United States within the meaning of the Espionage Act, USC 5031 and 5042. The transmission or the revelation of its contents in any manner to an unauthorized person is prohibited by law. Information so classified may be imparted only to persons in the military and naval services of the United States, appropriate civilian officers and employees of the Federal Government who have a legitimate interest therein, and to United States citizens of known loyalty and discretion who of necessity must be informed thereof.

NATIONAL ADVISORY COMMITTEE  
FOR AERONAUTICS

WASHINGTON

May 19, 1950

CONFIDENTIAL

CLASSIFICATION CHANGED

To UNCLASSIFIED

*naca Res. also*  
By authority of *RM-115*  
Date *5-8-57*

*at 5-23-57*



## NATIONAL ADVISORY COMMITTEE FOR AERONAUTICS

## RESEARCH MEMORANDUM

## FLIGHT MEASUREMENTS WITH THE DOUGLAS D-558-II

(BuAero No. 37974) RESEARCH AIRPLANE

## STATIC LATERAL AND DIRECTIONAL STABILITY CHARACTERISTICS

AS MEASURED IN SIDESLIPS AT MACH NUMBERS UP TO 0.87


By S. A. Sjöberg

## SUMMARY

Flight measurements were made in sideslips of the static lateral and directional stability characteristics of the Douglas D-558-II (BuAero No. 37974) research airplane. The directional stability of the airplane was positive in both the clean and landing conditions at all test speeds. About  $2^\circ$  of rudder deflection were required to produce  $1^\circ$  of sideslip in both the clean and landing conditions. There was no decrease in the effectiveness of the rudder in producing sideslip up to the highest Mach number reached (0.87). There was a considerable increase in dihedral effect with increase in normal-force coefficient;  $d\delta_a/d\beta$  increased from 1.0 at a normal-force coefficient of 0.10 to 3.1 at a normal-force coefficient of 0.90. At a constant value of normal-force coefficient the dihedral effect was the same in the landing condition as in the clean condition.

## INTRODUCTION

The National Advisory Committee for Aeronautics is conducting a flight research program utilizing the Douglas D-558-II (BuAero No. 37974) research airplane. The D-558-II airplanes were designed for flight research in the transonic speed range and were procured for the NACA by the Bureau of Aeronautics, Department of the Navy. The flight research program currently being conducted with the BuAero No. 37974 airplane consists of determining the stability and control characteristics and the aerodynamic loads acting on the wing and horizontal tail of the airplane from the stalling speed up to a maximum Mach number of



about 0.90. This paper presents results obtained on the static lateral and directional stability characteristics as measured in sideslips. Sideslip data are presented for the airplane in both the landing condition and clean condition for a Mach number range from 0.27 to 0.87. References 1 and 2 present results which have been obtained during the present flight program on other aerodynamic characteristics of the D-558-II airplane.

### AIRPLANE

The Douglas D-558-II airplanes have sweptback wing and tail surfaces and were designed for combination turbojet and rocket power. The airplane being used in the present investigation (BuAero No. 37974) does not yet have the rocket engine installed. This airplane is powered solely by a J-34-WE-40 turbojet engine which exhausts out of the bottom of the fuselage between the wing and the tail. Photographs of the airplane are shown as figures 1 and 2 and a three-view drawing is shown in figure 3. Pertinent airplane dimensions and characteristics are listed in table 1.

Both slats and fences are incorporated on the wing of the airplane. The wing slats can be locked in the closed position or they can be unlocked. When the slats are unlocked the slat position is a function of the angle of attack of the airplane. Also, the slats on the left and right wings are interconnected and therefore, at any time, have the same position. A section of the slat and the forward portion of the wing showing the motion of the slat with respect to the wing is shown in figure 4.

The airplane is equipped with an adjustable stabilizer but no means are provided for trimming out aileron or rudder control forces. No aerodynamic-balance or control-force booster system is used on any of the controls. Hydraulic dampers are installed on all control surfaces to aid in preventing any control-surface flutter. Dive brakes are located on the rear portion of the fuselage.

The variations of aileron and elevator position with control-wheel position are shown in figures 5 and 6, respectively, and the variation of rudder position with right-rudder-pedal position is shown in figure 7. The friction in the aileron, elevator, and rudder control systems as measured on the ground under no load are presented in figures 8, 9, and 10. These friction measurements were obtained by measuring the control position and the control force as the control was deflected slowly. The rates of control-surface deflection during the friction measurements were sufficiently low so that the control forces resulting from the hydraulic dampers in the control system were negligible.

## INSTRUMENTATION

Standard NACA recording instruments were installed in the airplane to measure the following quantities:

- Airspeed
- Altitude
- Elevator- and aileron-wheel forces
- Rudder pedal force
- Normal, longitudinal, and transverse accelerations
- Rolling, pitching, and yawing velocities
- Sideslip angle
- Stabilizer, elevator, rudder, left- and right-aileron, and slat positions

Strain gages were installed in the airplane to measure wing and tail loads. The strain-gage deflections were recorded on an oscillograph. All instruments were synchronized by means of a common timer.

A free-swiveling airspeed head was used to measure both static and total pressure. This airspeed head was mounted on a boom 7 feet forward of the nose of the airplane. A vane which was used to measure sideslip angle was mounted below the same boom  $4\frac{1}{2}$  feet forward of the nose of the airplane. (See fig. 1.)

The left- and right-aileron positions were measured on bell cranks about 1 foot forward of the ailerons and the slat position was measured on the slat control cable in the fuselage. The stabilizer, rudder, and elevator positions were measured on the control surfaces. The elevator position presented in this paper is the average of two measured positions. One measuring point was 6 inches outboard of the vertical stabilizer and the other 11 inches inboard of the tip of the horizontal tail measured perpendicular to the airplane center line. In no case was the difference between the two measurements greater than  $0.3^\circ$ . Thus, for the airplane flight conditions covered in this paper, the twist of the elevator with respect to the horizontal stabilizer was small. The elevator positions presented were measured with respect to the stabilizer and the stabilizer position was measured with respect to the fuselage center line. The slat position as used in this paper is defined in figure 4 by the distance  $d_s$ . All control positions were measured perpendicular to the control hinge line.

## AIRSPEED CALIBRATION

The calibration of the airspeed installation was accomplished in the Mach number range from 0.30 to 0.70 by making tower passes. The details of the tower-pass method of obtaining airspeed calibrations are given in reference 3. In order to extend the calibration up to a Mach number of 0.90 the following procedure was used: The blocking error due to the fuselage was assumed to be constant. For the combination of fuselage shape and airspeed-boom length used this assumption is justified on the basis of results reported in reference 4. The blocking error due to the airspeed head itself was established up to a Mach number of 0.85 from wind-tunnel tests. By combining the constant blocking error of the fuselage with the blocking error due to the airspeed head, the airspeed calibration was extended up to a Mach number of 0.85. For Mach numbers between 0.85 and 0.90 the calibration was extrapolated. The Mach numbers given in this paper are believed accurate to  $\pm 0.01$ .

## TESTS, RESULTS, AND DISCUSSION

The static lateral and directional stability characteristics were measured in sideslips at various speeds with the airplane in both the clean and the landing configurations. With the airplane in the clean condition (flaps up, gear up, slats locked, duct flaps closed), sideslips were made at five different Mach numbers in the range from 0.34 to 0.87. In the landing condition (flaps down, gear down, slats unlocked, duct flaps open), sideslips were made at indicated airspeeds of 158 and 182 miles per hour. All of the data presented, except that at a Mach number of 0.34 with the airplane in the clean condition, were obtained as the sideslip angle was slowly increased. The data at a Mach number of 0.34 were obtained at substantially constant sideslip angles. For the runs in which the sideslip angle was increasing, the rate of change of the sideslip angle was between  $0.1^\circ$  per second and  $0.4^\circ$  per second. The data were obtained in the altitude range from 13,000 to 21,000 feet.

Figure 11 shows the variations of rudder, total aileron, and elevator control positions and control forces and angle of bank with sideslip angle for the airplane in the clean condition. Similar data for the airplane in the landing condition are shown in figure 12. Also included in figure 12 is the slat position.

The directional stability of the airplane was positive in both the clean and landing conditions at all test speeds. About  $2^\circ$  of rudder deflection were required to produce  $1^\circ$  of sideslip in both the clean

and landing conditions, thus indicating no change in the directional stability occurred in going from the clean to the landing condition. In figure 13 the slopes of the curves of rudder position against sideslip angle  $d\delta_r/d\beta$  from figure 11 are plotted as a function of Mach number. The values of  $d\delta_r/d\beta$  were measured for a sideslip-angle range of  $\pm 2^\circ$ . Up to the highest Mach number reached (0.87), there has been no decrease in the effectiveness of the rudder in producing sideslip since  $d\delta_r/d\beta$  is substantially constant up to this Mach number. The rudder-free directional stability, as measured by the variation of rudder pedal force with the sideslip angle, was positive for all conditions investigated.

The curves of aileron position against sideslip angle in figures 11 and 12 show a considerable increase in dihedral effect with increase in normal-force coefficient. This increase is also shown in figure 14, where the variations of aileron angle with sideslip angle  $d\delta_a/d\beta$ , as obtained from figures 11 and 12, are plotted against normal-force coefficient. Data are included for both the clean and landing conditions. The values of  $d\delta_a/d\beta$  were measured for a sideslip-angle range of  $\pm 2^\circ$ . The dihedral effect  $d\delta_a/d\beta$  increases from 1.0 at a normal-force coefficient of 0.10 to 3.1 at a normal-force coefficient of 0.90. Figure 14 also shows that at a given normal-force coefficient the dihedral effect is the same in the landing condition as in the clean condition. Figures 11 and 12 show that the pitching moment due to sideslip, as measured by the variation of elevator deflection required for trim with sideslip angle, is small for all conditions investigated.

Inspection of the control-force curves of figures 11 and 12 shows that the curves are sometimes discontinuous near zero sideslip. The discontinuities are probably caused by the friction in the control system. When the control forces due to the aerodynamic hinge moments are large, this friction effect is masked. The slat-position measurements presented in figure 12 show that the slat position during the left and right sideslips was not the same. The reason for the difference in slat positions is not known.

#### CONCLUDING REMARKS

Flight measurements were made in sideslips of the static lateral and directional stability characteristics of the Douglas D-558-II (BuAero No. 37974) research airplane. The directional stability of the airplane was positive in both the clean and landing conditions at all test speeds. About  $2^\circ$  of rudder deflection were required to produce  $1^\circ$  of sideslip in both the clean and landing conditions. There was no

decrease in the effectiveness of the rudder in producing sideslip up to the highest Mach number reached (0.87). There was a considerable increase in dihedral effect with increase in normal-force coefficient;  $d\delta_a/d\beta$  increased from 1.0 at a normal-force coefficient of 0.10 to 3.1 at a normal-force coefficient of 0.90. At a constant value of normal-force coefficient the dihedral effect is the same in the landing condition as in the clean condition.

Langley Aeronautical Laboratory  
National Advisory Committee for Aeronautics  
Langley Air Force Base, Va.

#### REFERENCES

1. Sjoberg, Sigurd A.: Preliminary Measurements of the Dynamic Lateral Stability Characteristics of the Douglas D-558-II (BuAero No. 37974) Airplane. NACA RM L9G18, 1949.
2. Sjoberg, S. A., and Champine, R. A.: Preliminary Flight Measurements of the Static Longitudinal Stability and Stalling Characteristics of the Douglas D-558-II Research Airplane (BuAero No. 37974). NACA RM L9H31a, 1949.
3. Thompson, F. L., and Zalovcik, John A.: Airspeed Measurements in Flight at High Speeds. NACA ARR, Oct. 1942.
4. Danforth, Edward C. B., and Johnston, J. Ford: Error in Airspeed Measurement Due to Static-Pressure Field ahead of Sharp-Nose Bodies of Revolution at Transonic Speeds. NACA RM L9C25, 1949.

TABLE 1

## DIMENSIONS AND CHARACTERISTICS OF THE

## DOUGLAS D-558-II AIRPLANE

## Wing:

Root airfoil section (normal to 0.30 chord) . . . . .	NACA 63-010
Tip airfoil section (normal to 0.30 chord) . . . . .	NACA 63 <sub>1</sub> -012
Total area, sq ft . . . . .	175.0
Span, ft . . . . .	25.0
Mean aerodynamic chord, in. . . . .	87.301
Root chord (parallel to plane of symmetry), in. . . . .	108.508
Tip chord (parallel to plane of symmetry), in. . . . .	61.180
Taper ratio . . . . .	0.565
Aspect ratio . . . . .	3.570
Sweep at 0.30 chord, deg . . . . .	35.0
Incidence at fuselage center line, deg . . . . .	3.0
Dihedral, deg . . . . .	-3.0
Geometric twist, deg . . . . .	0
Total aileron area (aft of hinge), sq ft . . . . .	9.8
Aileron travel (each), deg . . . . .	±15
Total flap area, sq ft . . . . .	12.58
Flap travel, deg . . . . .	50

## Horizontal tail:

Root airfoil section (normal to 0.30 chord) . . . . .	NACA 63-010
Tip airfoil section (normal to 0.30 chord) . . . . .	NACA 63-010
Area (including fuselage), sq ft . . . . .	39.9
Span, in. . . . .	143.6
Mean aerodynamic chord, in. . . . .	41.75
Root chord (parallel to plane of symmetry) . . . . .	53.6
Tip chord (parallel to plane of symmetry) . . . . .	26.8
Taper ratio . . . . .	0.50
Aspect ratio . . . . .	3.59
Sweep at 0.30 chord line, deg . . . . .	40.0
Dihedral, deg . . . . .	0
Elevator area, sq ft . . . . .	9.4
Elevator travel . . . . .	
Up, deg . . . . .	25
Down, deg . . . . .	15



TABLE 1 -- Concluded

## DIMENSIONS AND CHARACTERISTICS OF THE

## DOUGLAS D-558-II AIRPLANE -- Concluded

## Vertical tail:

Airfoil section (parallel to fuselage center line) . . . .	NACA 63-010
Area, sq ft . . . . .	36.6
Height from fuselage center line, in. . . . .	98.0
Root chord (parallel to fuselage center line), in. . . . .	146.0
Tip chord (parallel to fuselage center line), in. . . . .	44.0
Sweep angle at 0.30 chord, deg . . . . .	49.0
Rudder area (aft of hinge line), sq ft . . . . .	6.15
Rudder travel, deg . . . . .	±25

## Fuselage:

Length, ft . . . . .	42.0
Maximum diameter, in. . . . .	60.0
Fineness ratio . . . . .	8.40
Speed-retarder area, sq ft . . . . .	5.25

Power plant . . . . . J-34-WE-40

2 jatos for take-off

Airplane weight (full fuel), lb . . . . .	10,645
Airplane weight (no fuel), lb . . . . .	9,085
Airplane weight (full fuel and 2 jatos), lb . . . . .	11,060

## Center-of-gravity locations:

Full fuel (gear down), percent mean aerodynamic chord . . . .	25.3
Full fuel (gear up), percent mean aerodynamic chord . . . . .	25.8
No fuel (gear down), percent mean aerodynamic chord . . . . .	26.8
No fuel (gear up), percent mean aerodynamic chord . . . . .	27.5
Full fuel and 2 jatos (gear down), percent mean aerodynamic chord . . . . .	29.2



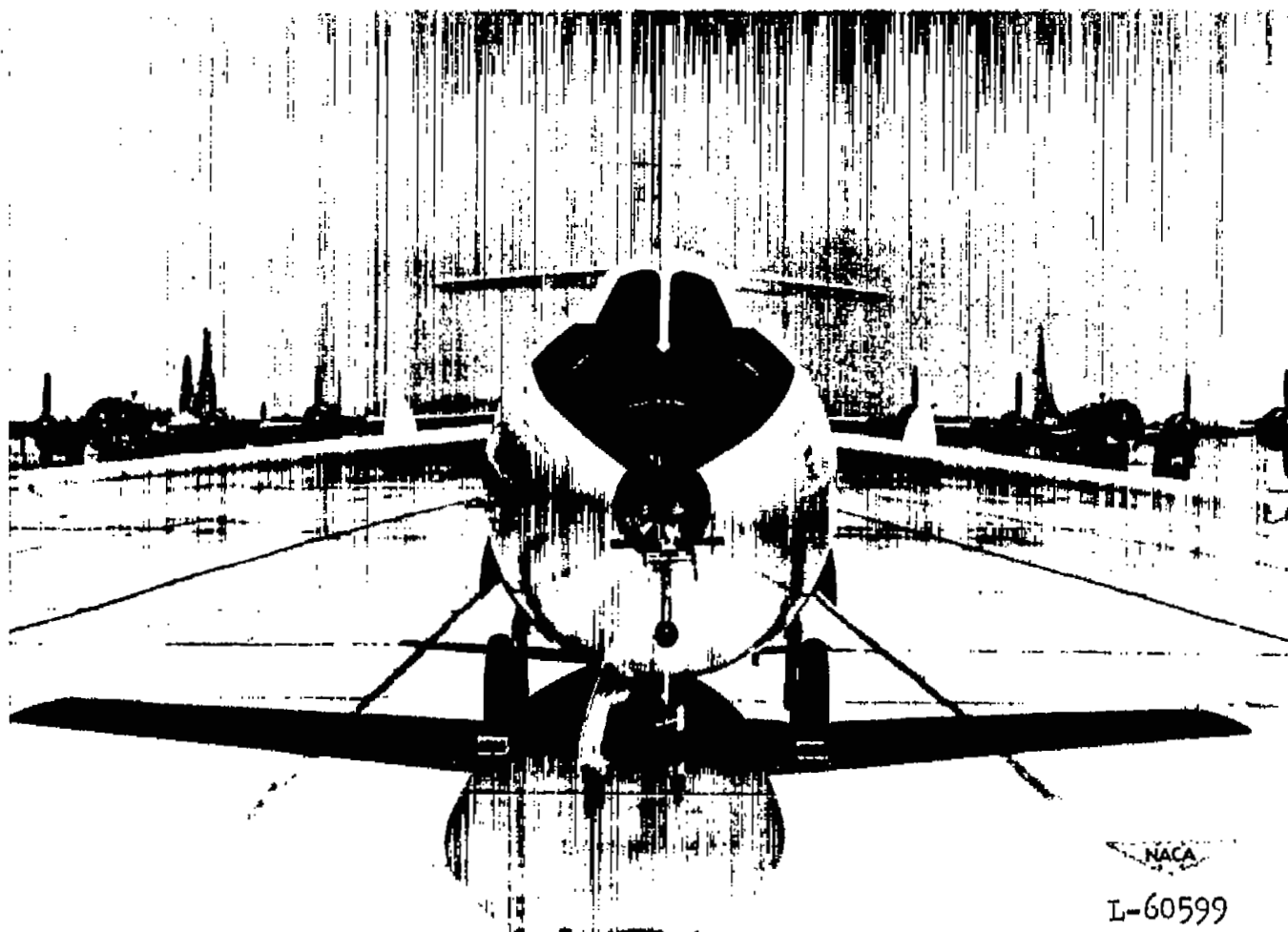


Figure 1.- Front view of Douglas D-558-II (BuAero No. 37974) research airplane.



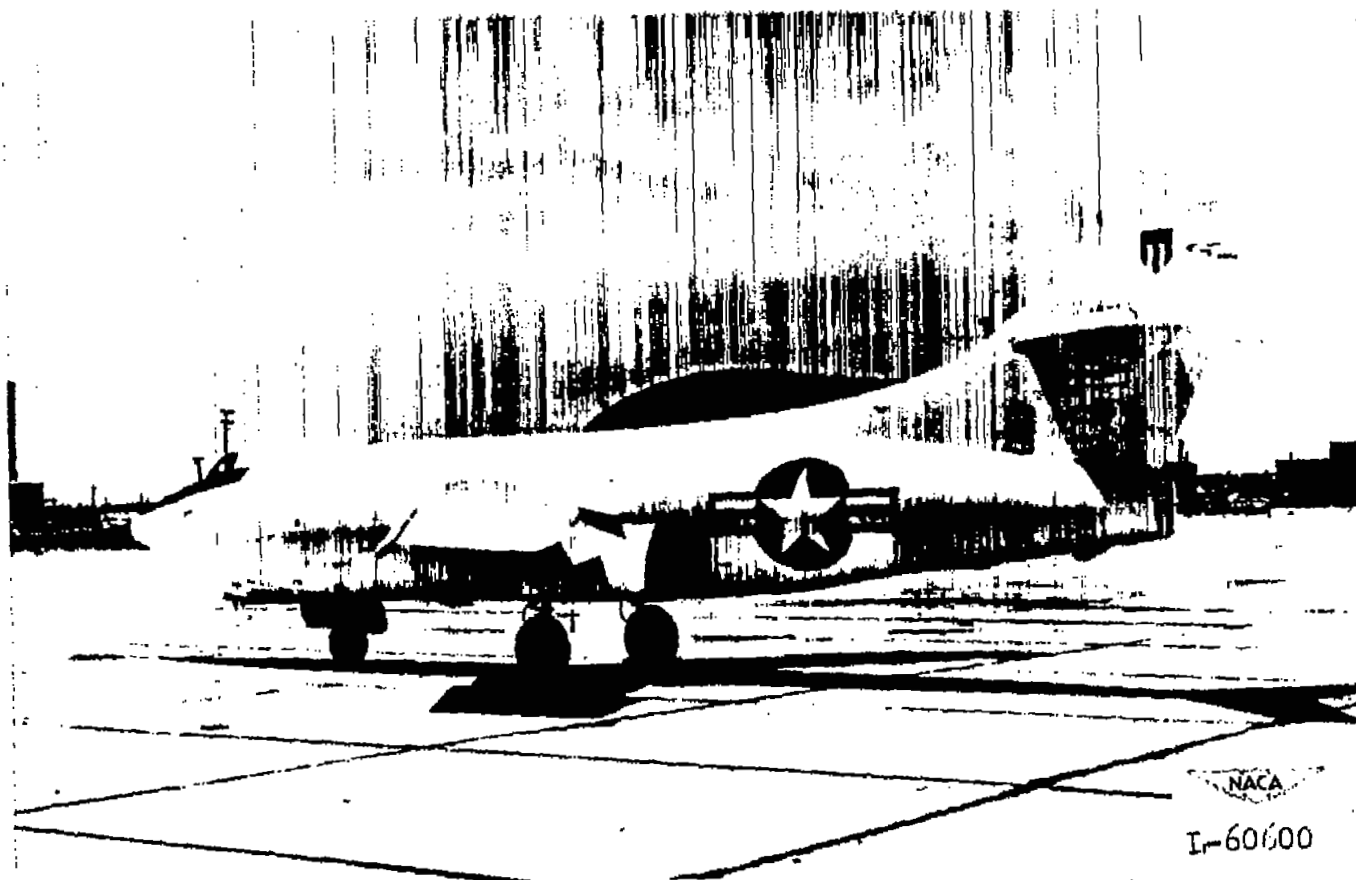


Figure 2.- Three-quarter rear view of Douglas D-558-II (BuAero No. 37974)  
research airplane.



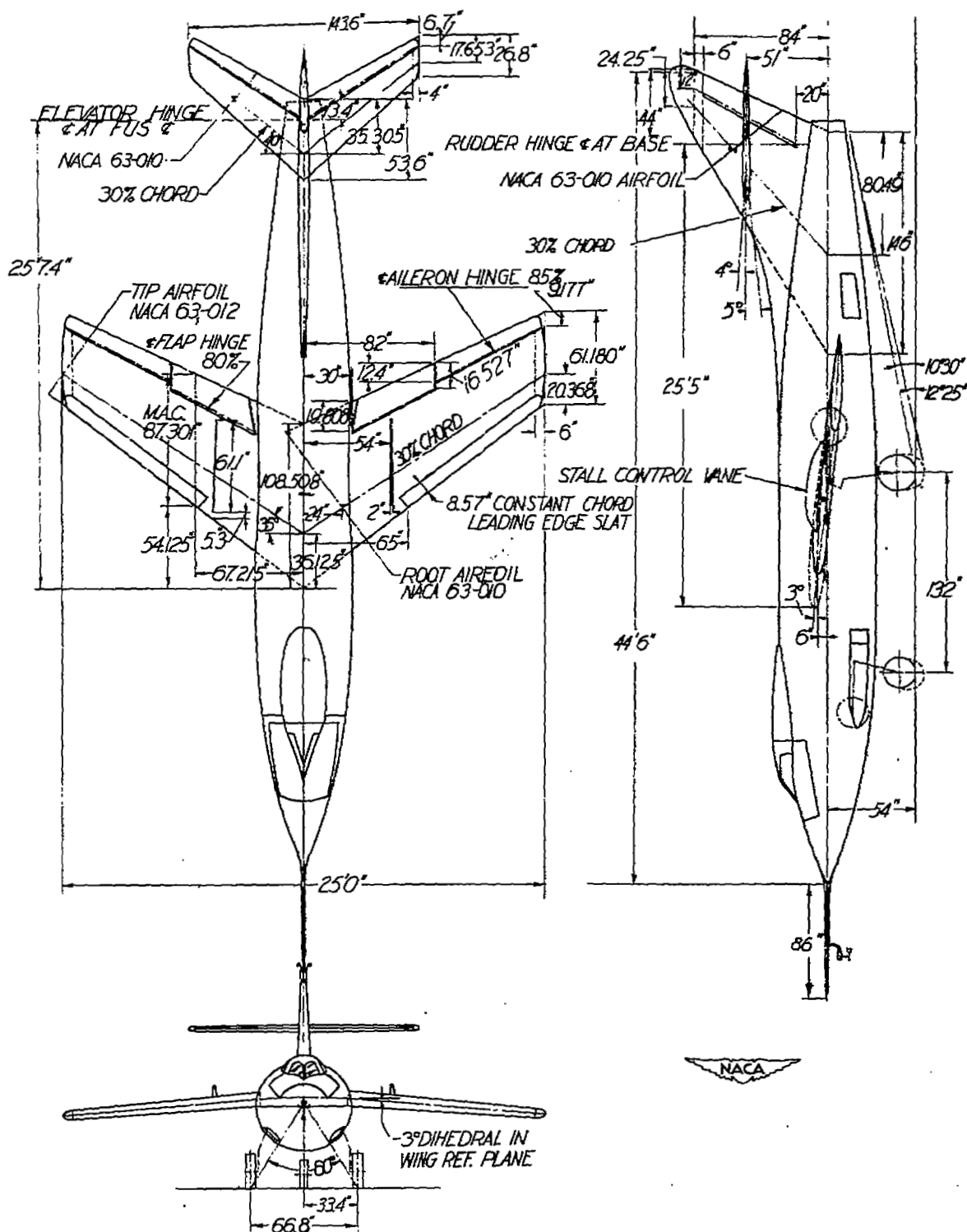


Figure 3.- Three-view drawing of the Douglas D-558-II (BuAero No. 37974) research airplane.

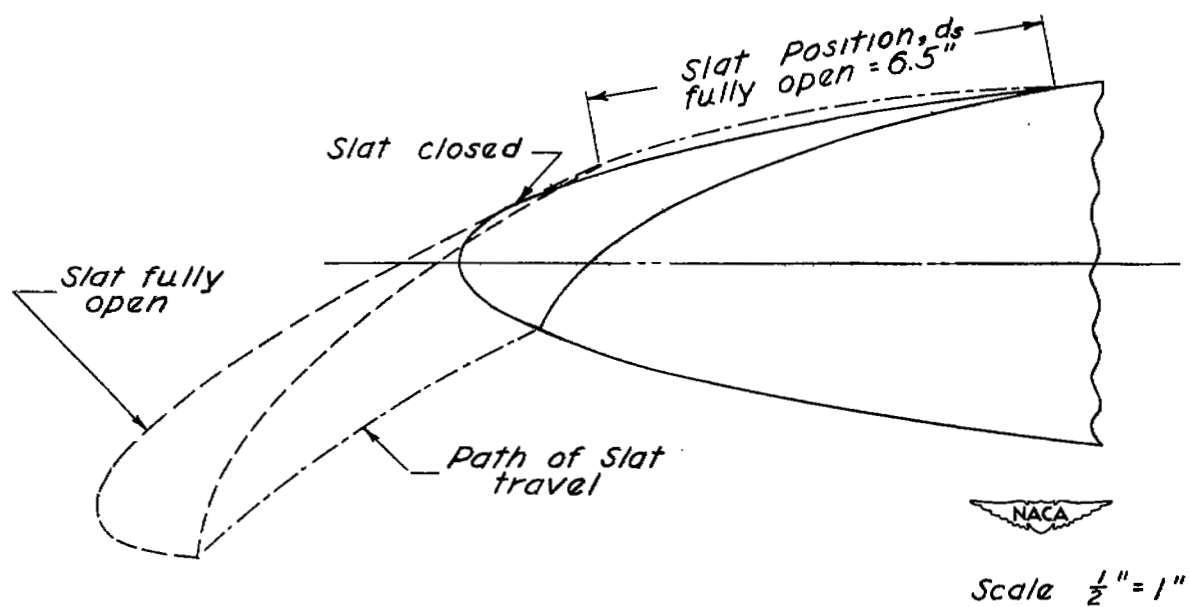


Figure 4.- Section of wing slat of Douglas D-558-II (BuAero No. 37974) research airplane perpendicular to leading edge of wing.

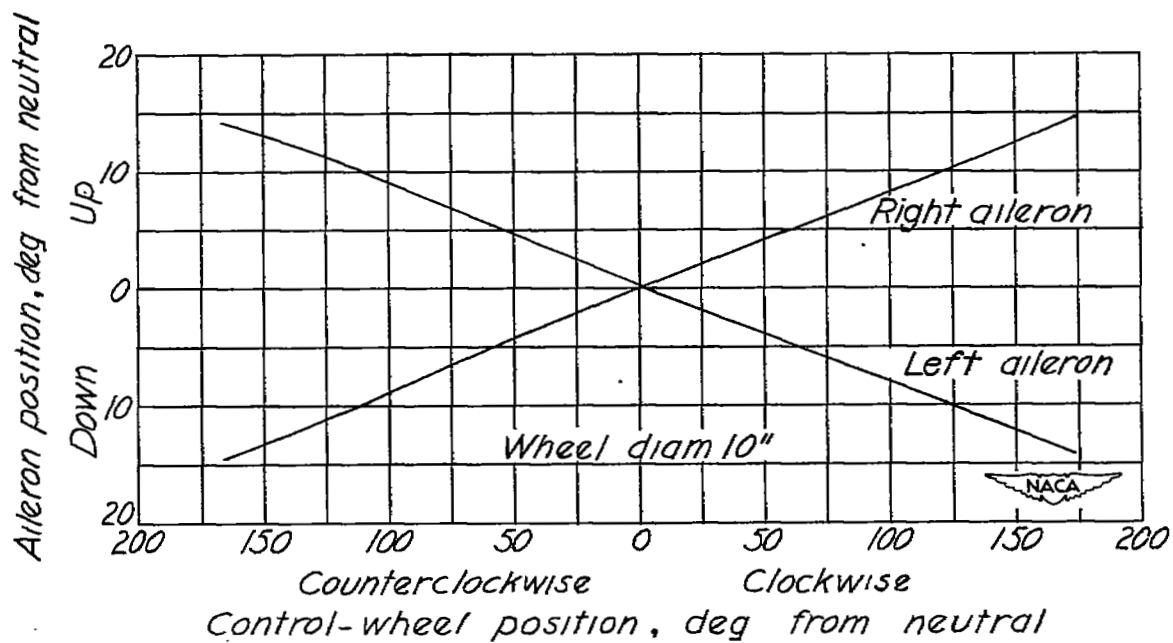


Figure 5.- Variation of left- and right-aileron positions with control-wheel position. No load on system.

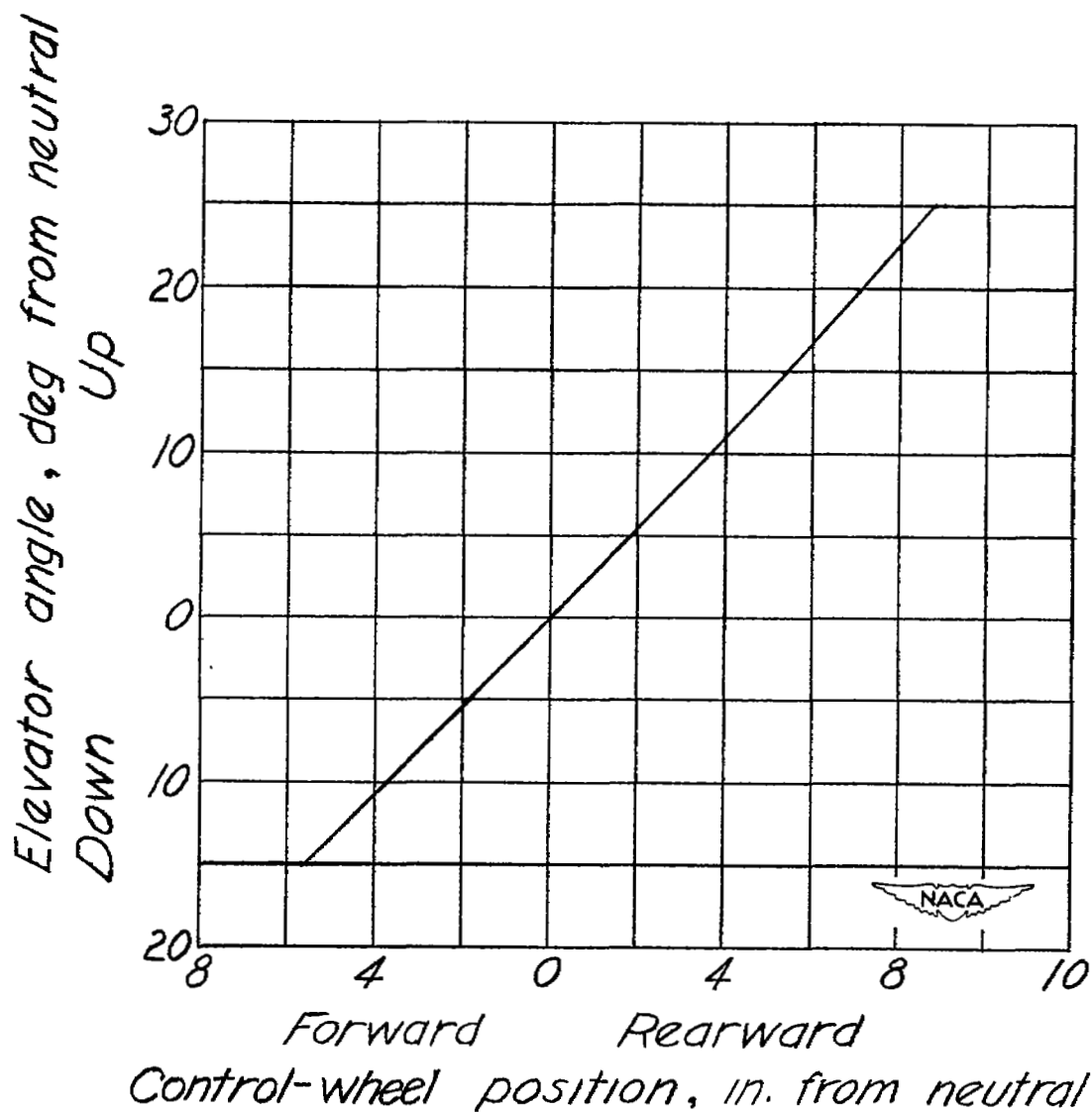


Figure 6.- Variation of elevator position with control-wheel position.  
No load on system.

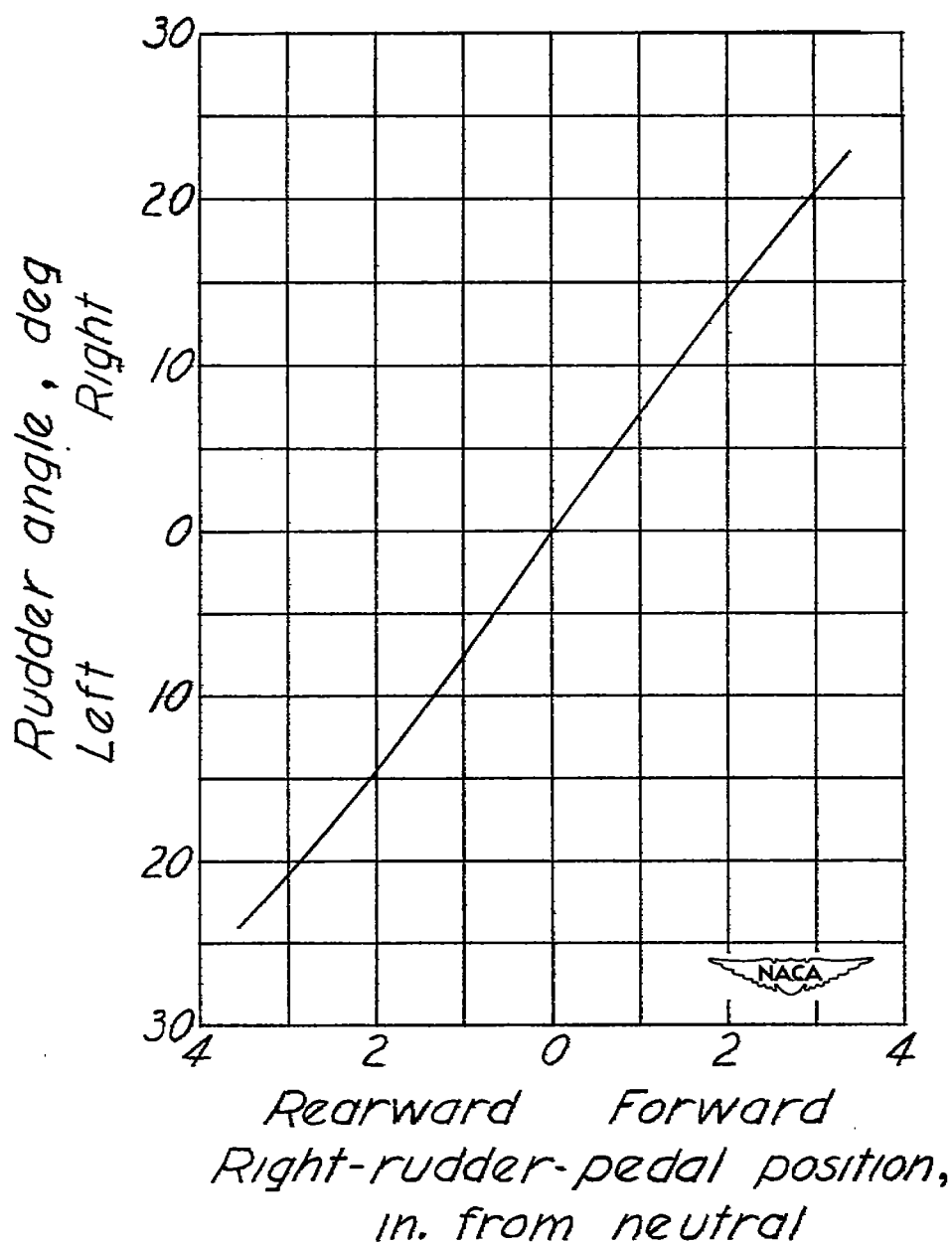


Figure 7.- Variation of rudder position with right-rudder-pedal position.  
No load on system.

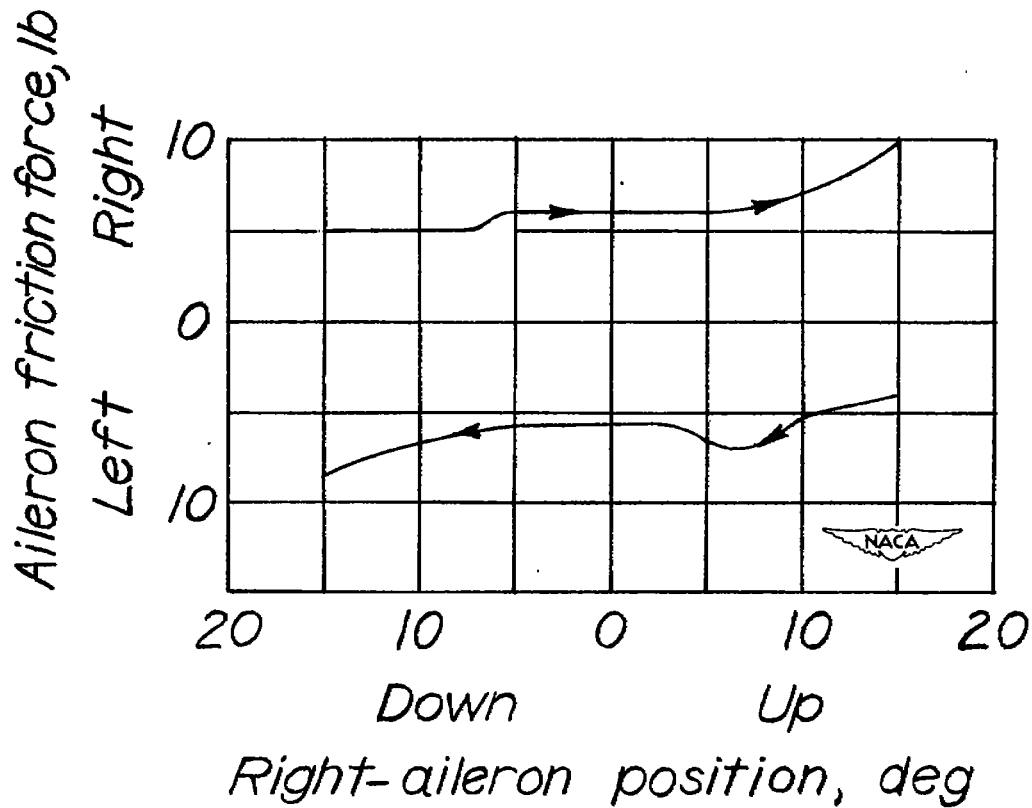


Figure 8.- Aileron control force required to deflect ailerons on the ground under no load.

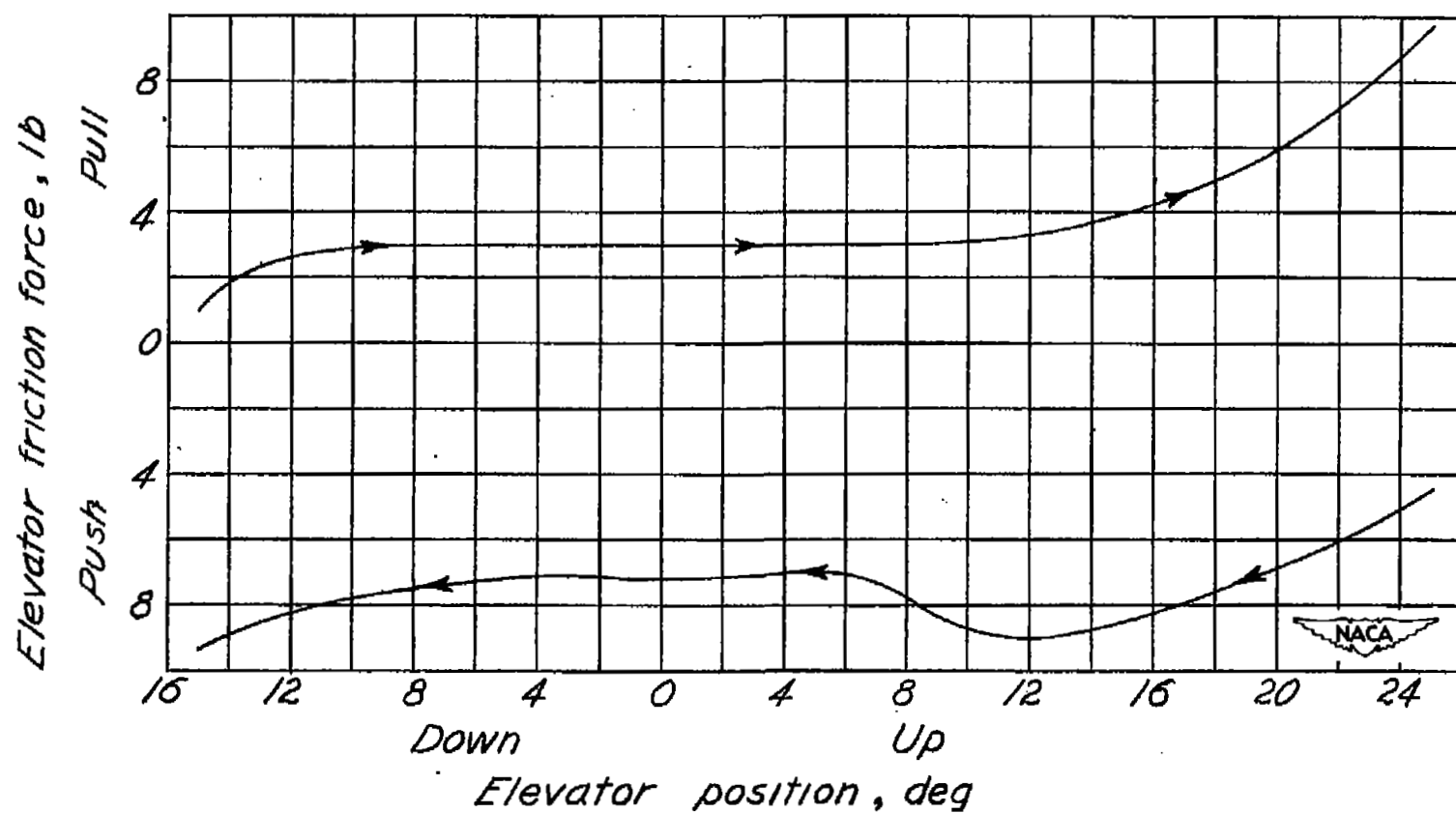


Figure 9.- Elevator control force required to deflect elevator on the ground under no load.

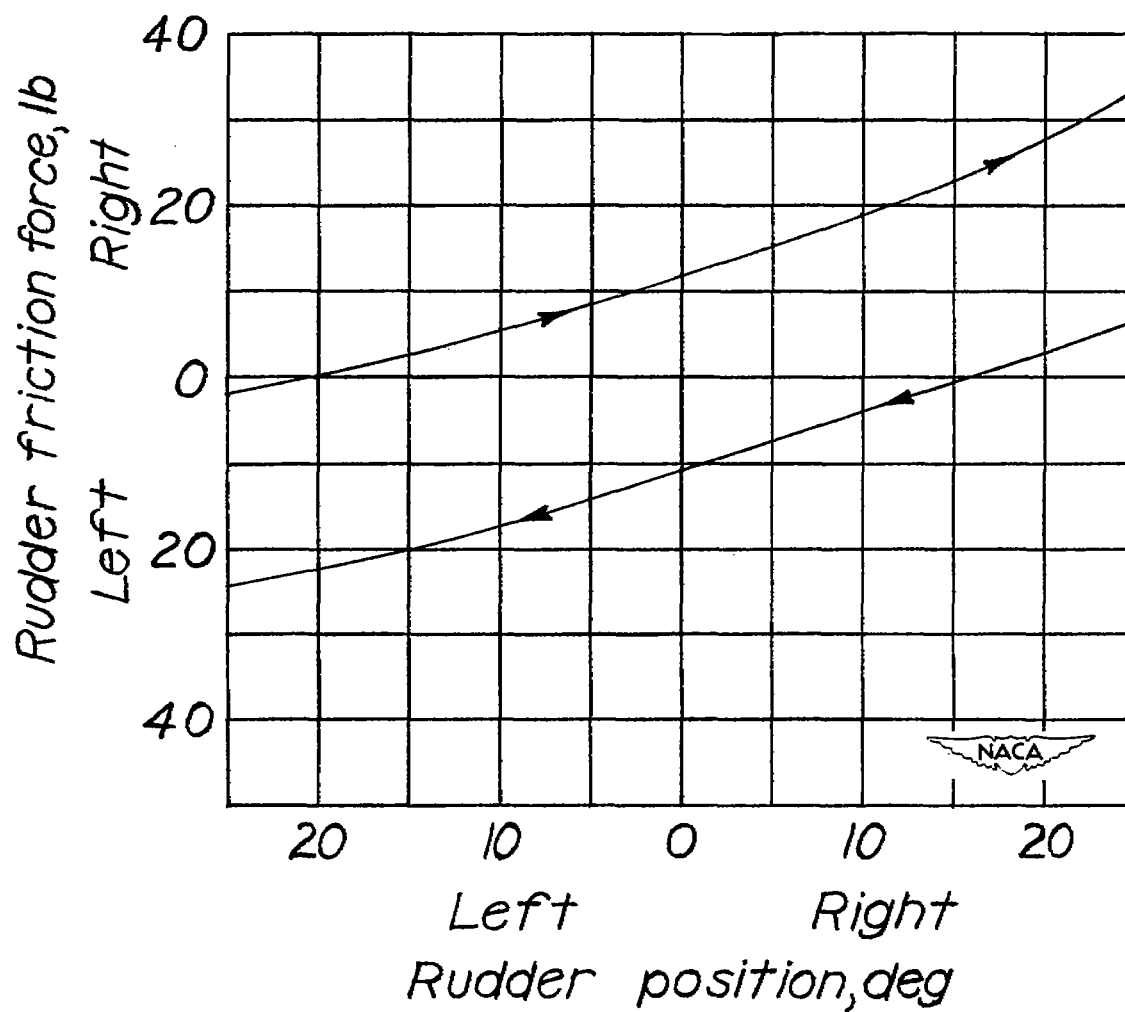
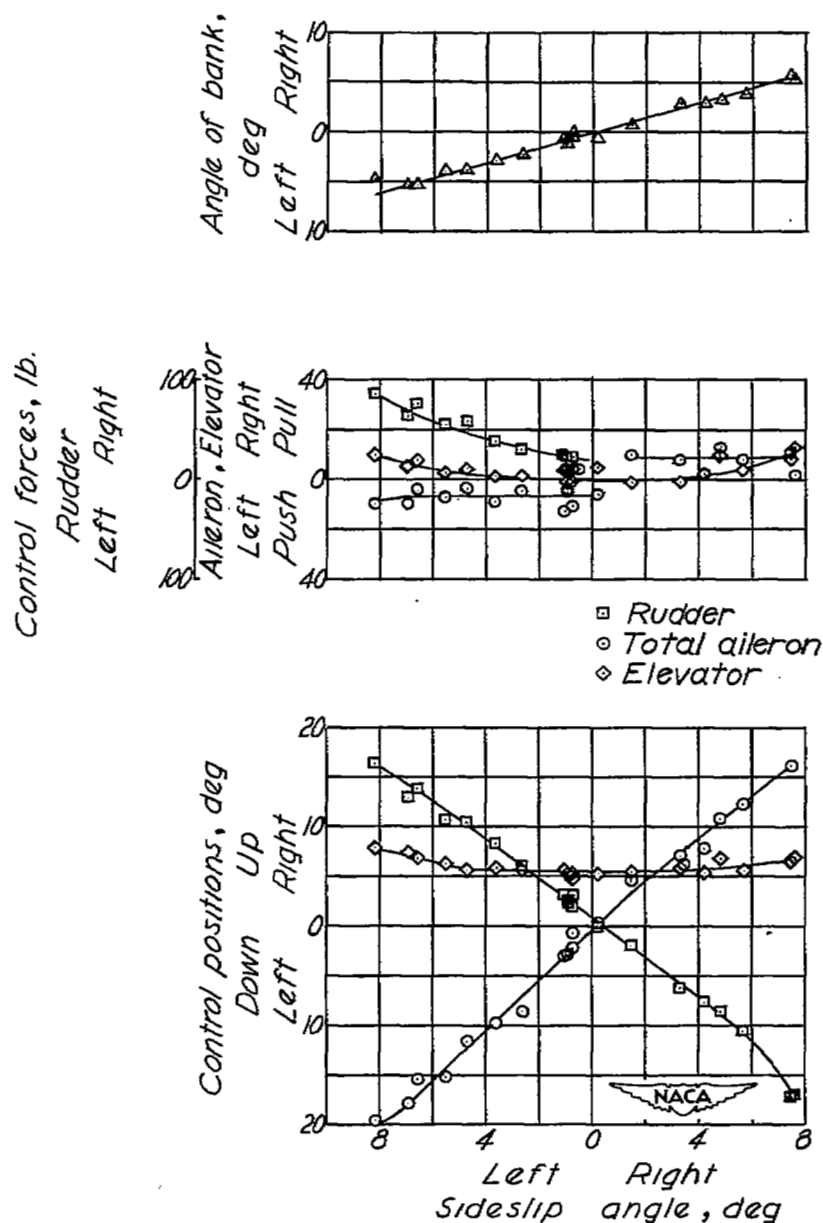
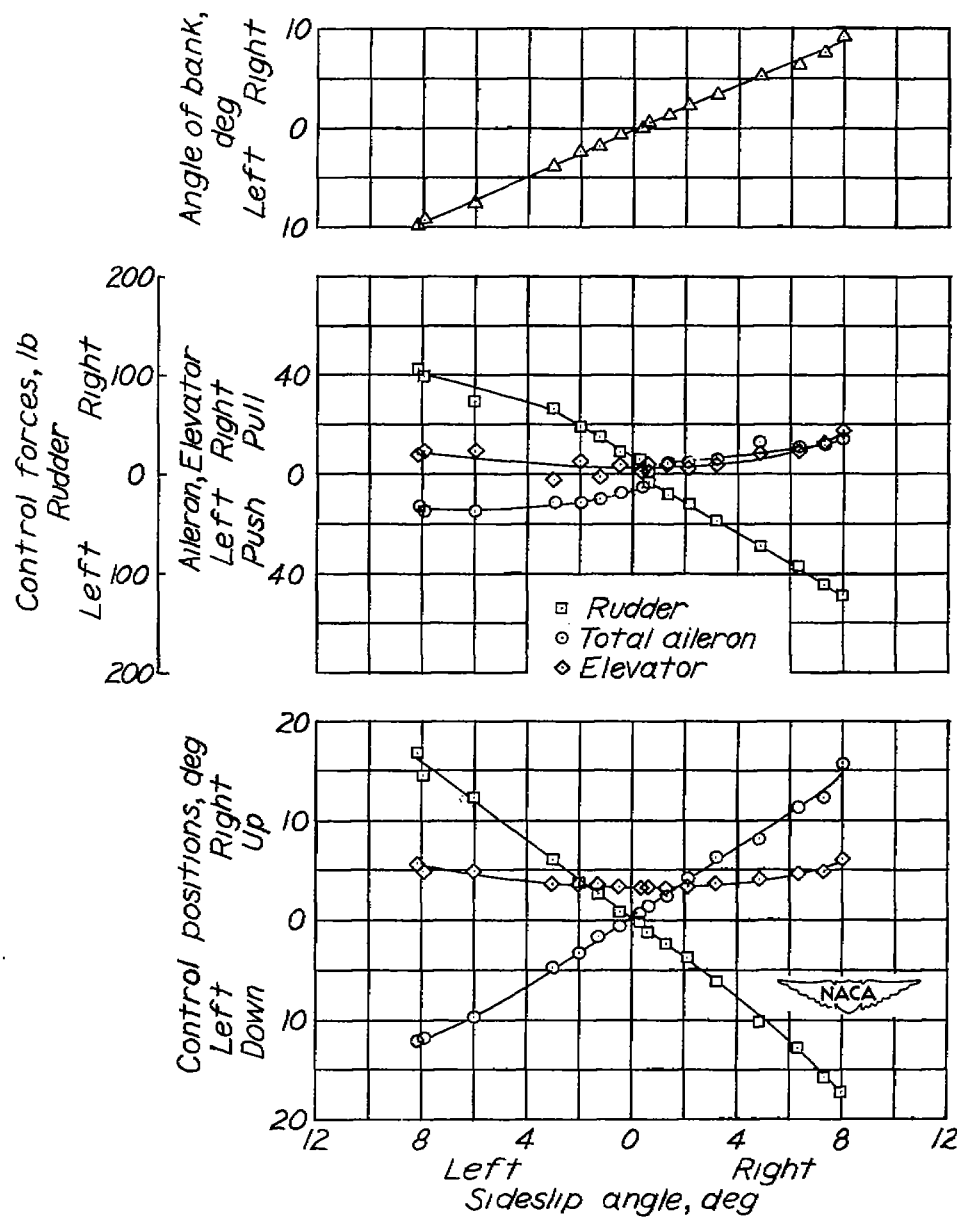


Figure 10.- Rudder control force required to deflect rudder on the ground under no load.



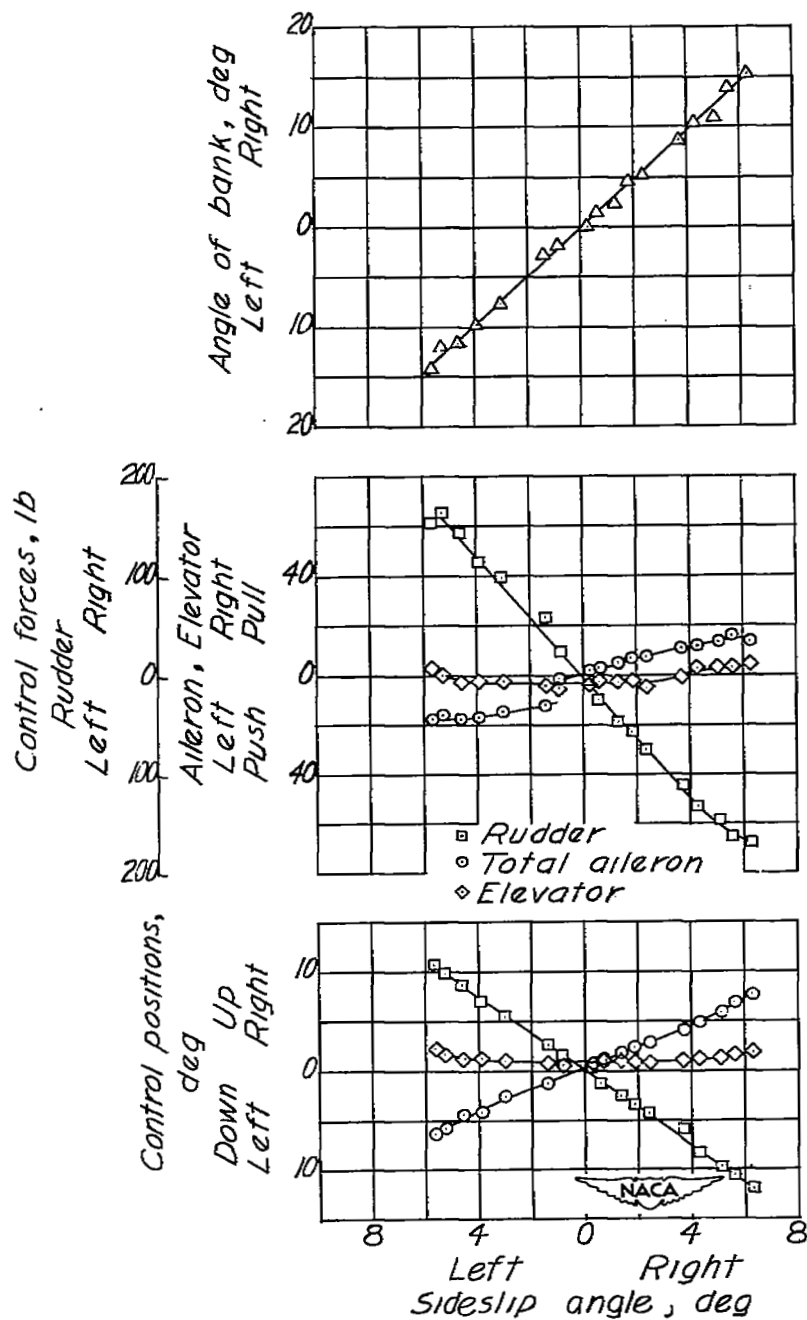
(a)  $V_c = 177$  miles per hour;  $M = 0.34$ ;  $C_N = 0.73$ ;  
 stabilizer setting,  $1.7^\circ$  leading edge up;  
 engine power, 11,000 rpm.

Figure 11.- Sideslip characteristics of the Douglas D-558-II (BuAero No. 37974) research airplane. Flaps up; gear up; slats locked; duct flaps closed.



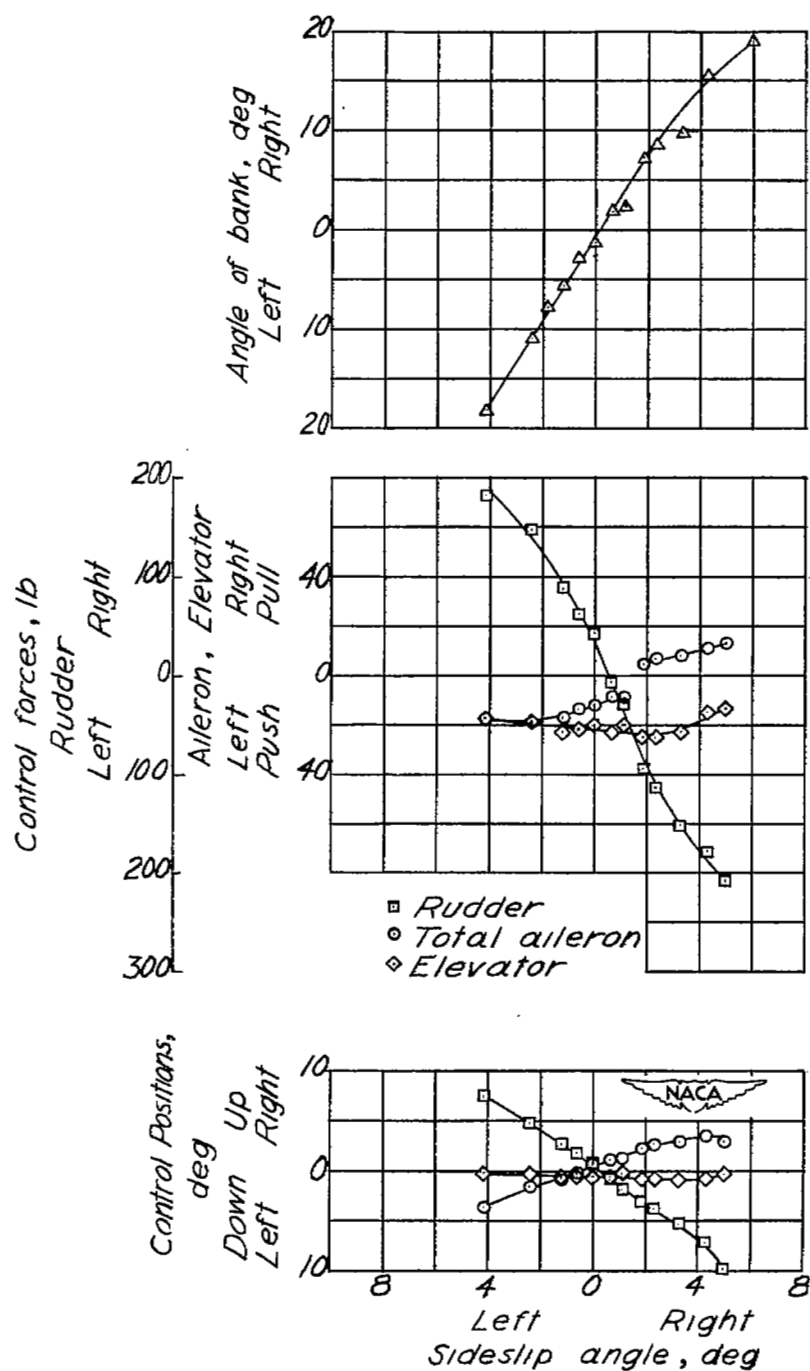
(b)  $V_c = 213$  miles per hour;  $M = 0.40$ ;  $C_N = 0.48$ ; stabilizer setting,  $1.7^\circ$  leading edge up; engine power, 11,000 rpm.

Figure 11.- Continued.



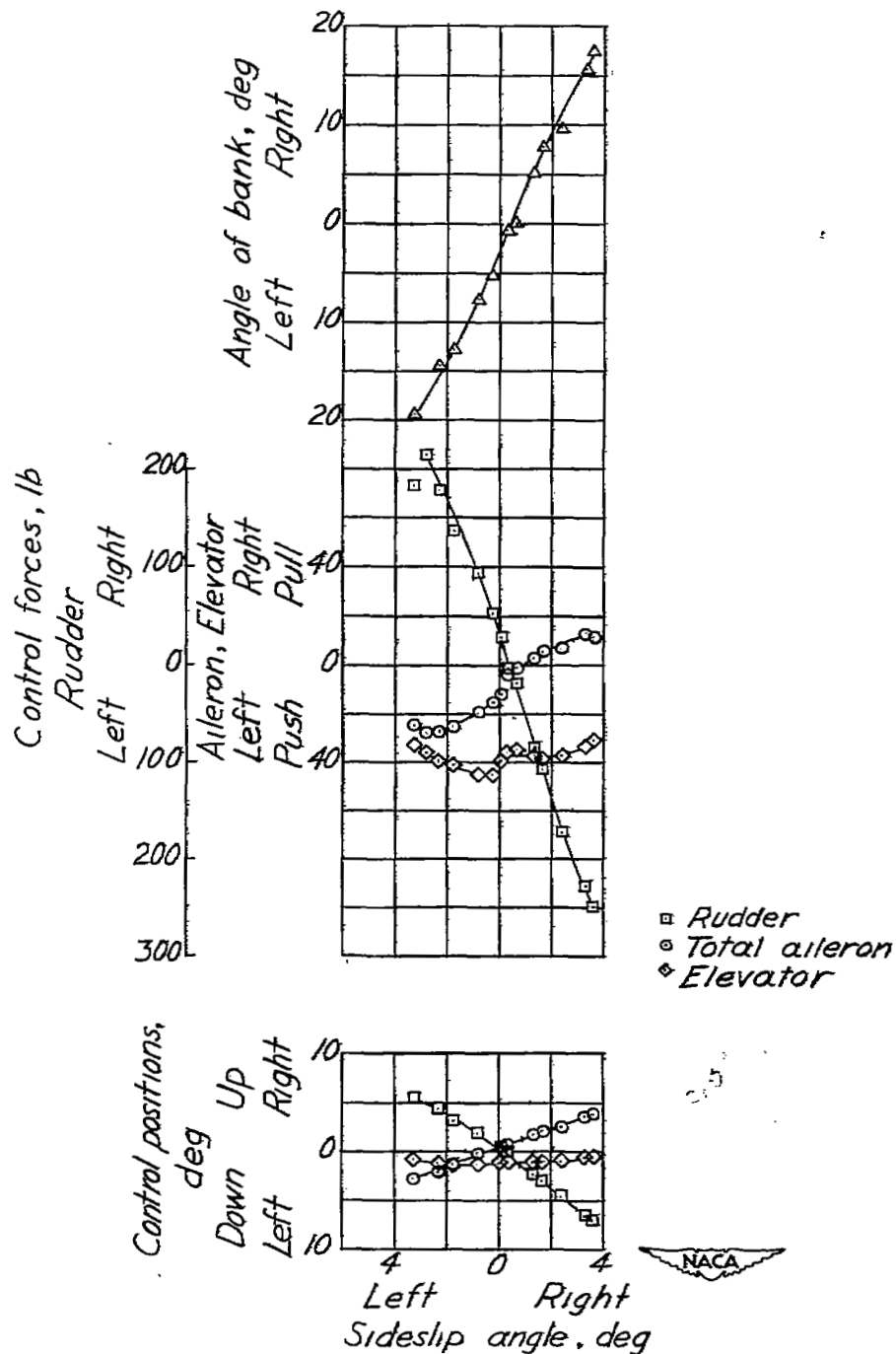
(c)  $V_c = 330$  miles per hour;  $M = 0.60$ ;  $C_N = 0.20$ ; stabilizer setting,  $1.8^\circ$  leading edge up; engine power, 11,400 rpm.

Figure 11.- Continued.



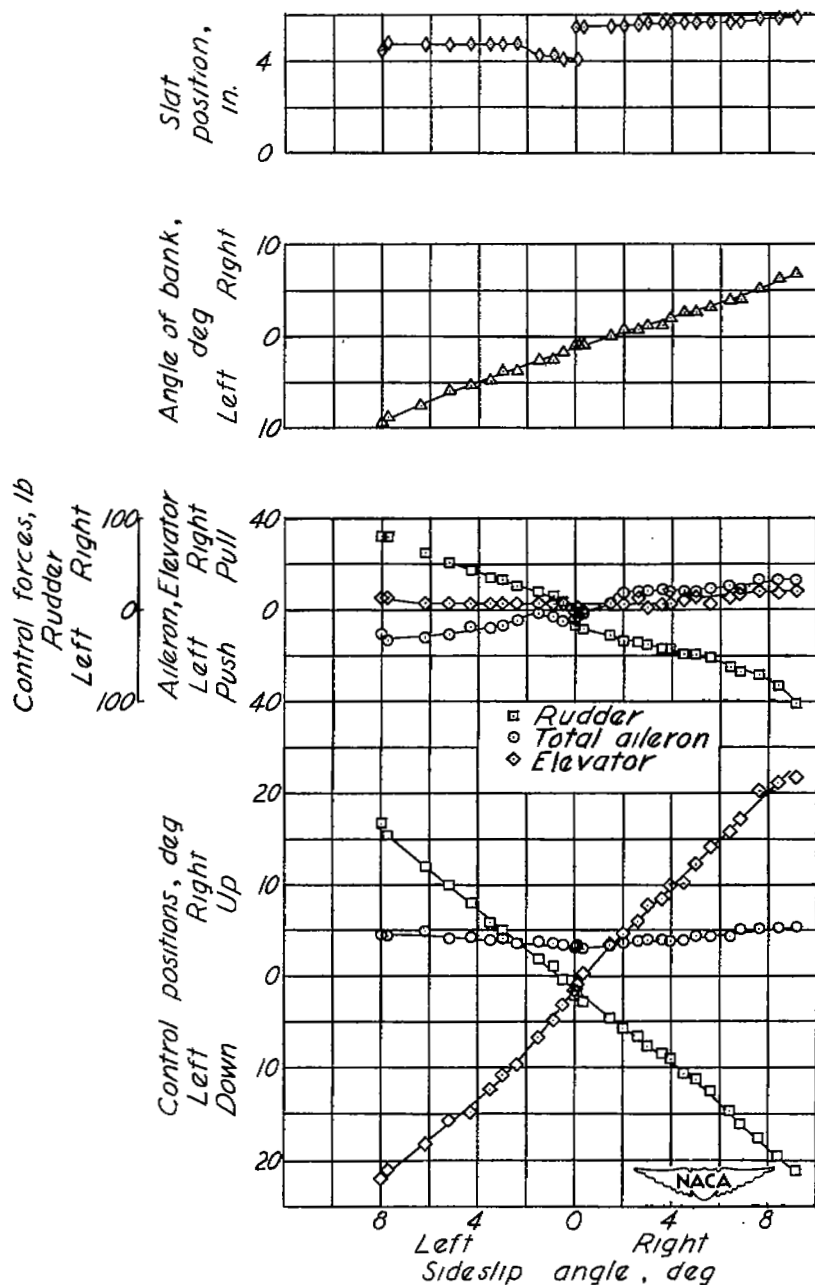
(d)  $V_C = 440$  miles per hour;  $M = 0.78$ ;  $C_N = 0.12$ ; stabilizer setting,  $1.7^\circ$  leading edge up; engine power, 12,300 rpm.

Figure 11.- Continued.



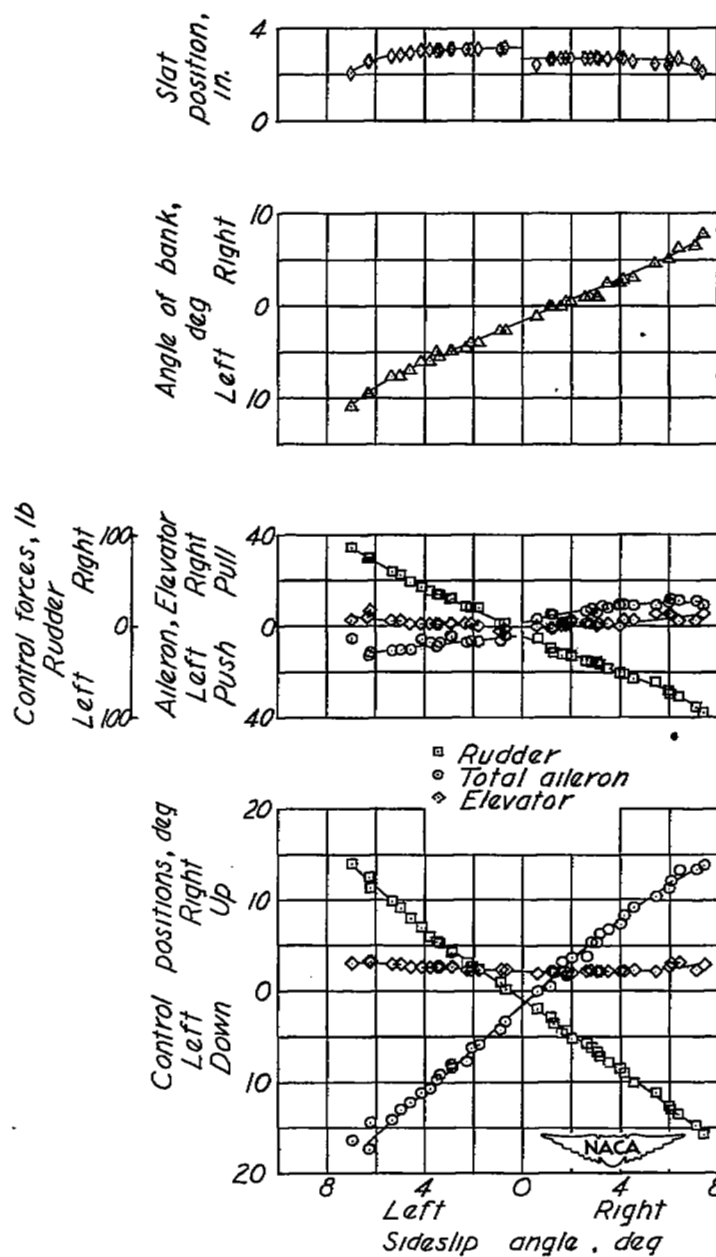
(e)  $V_C = 494$  miles per hour;  $M = 0.87$ ;  $C_N = 0.10$ ; stabilizer setting,  $1.8^\circ$  leading edge up; engine power, 12,500 rpm.

Figure 11.- Concluded.



(a)  $V_c = 158$  miles per hour;  $M = 0.27$ ;  $C_N = 0.91$ ;  
 stabilizer setting,  $1.9^\circ$  leading edge up;  
 engine power, 11,400 rpm.

Figure 12.- Sideslip characteristics of the Douglas D-558-II (BuAero No. 37974) research airplane. Flaps down; gear down; slats unlocked; duct flaps open.



(b)  $V_C = 182$  miles per hour;  $M = 0.34$ ;  $C_N = 0.71$ ; stabilizer setting,  $1.9^\circ$  leading edge up; engine power, 11,400 rpm.

Figure 12.- Concluded.

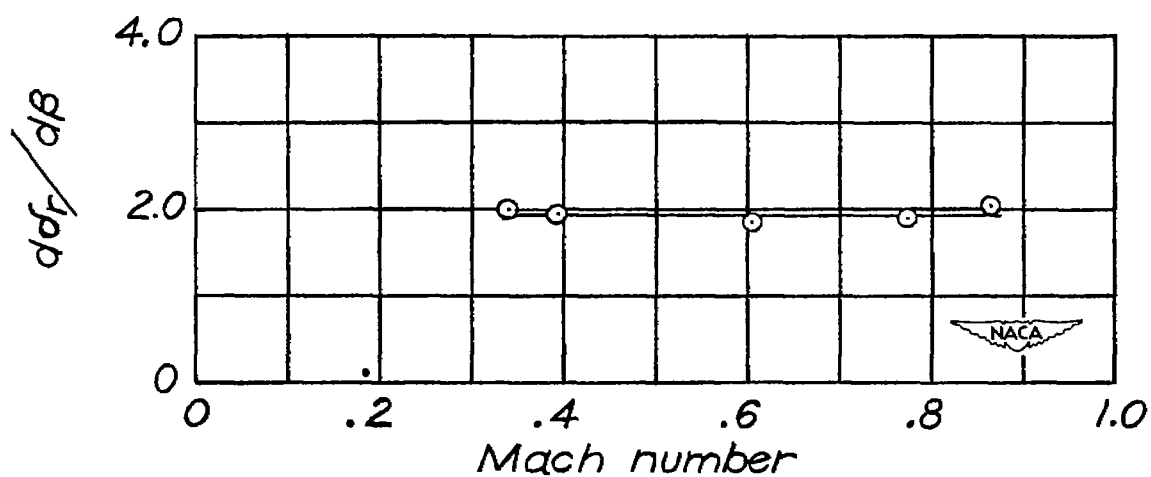


Figure 13.- Variation of  $d\delta_r/d\beta$  with Mach number  $M$  as measured in sideslips with the Douglas D-558-II (BuAero No. 37974) research airplane. Flaps up; gear up; slats locked; duct flaps closed.

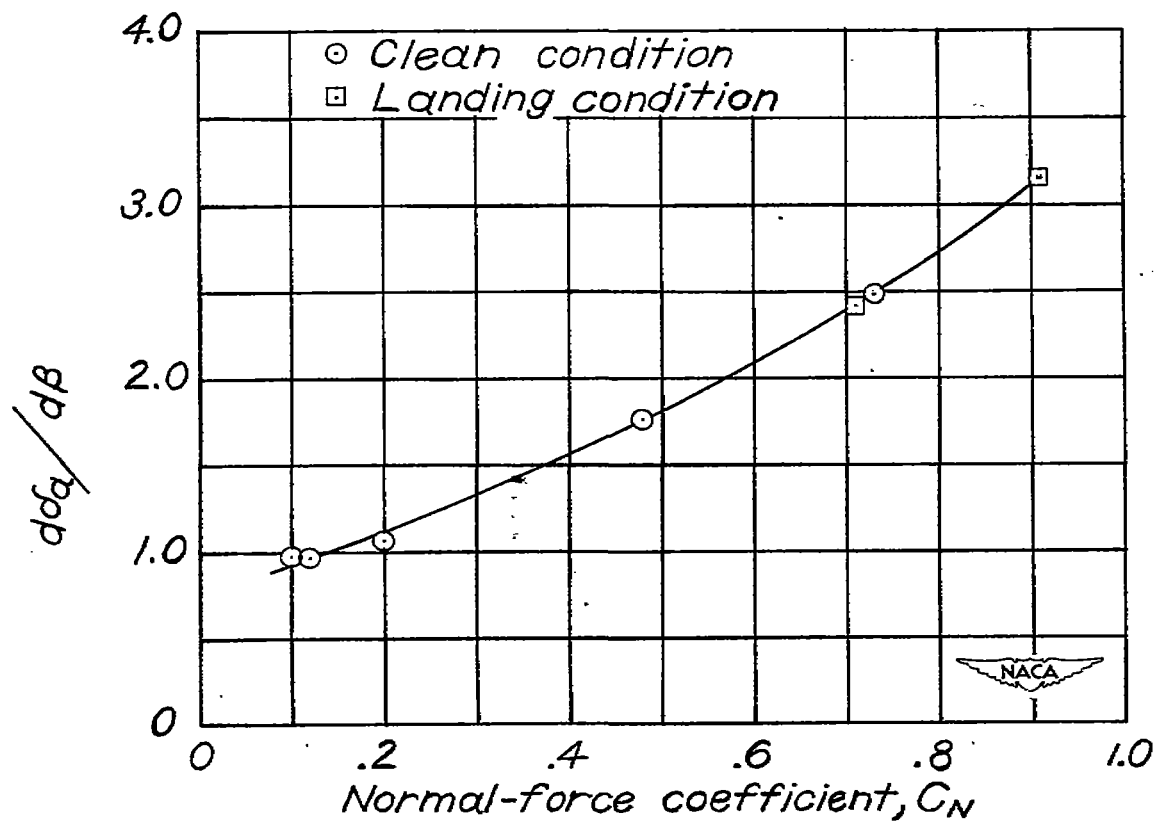


Figure 14.- Variation of  $d\delta_a/d\beta$  with normal-force coefficient  $C_N$  as measured in sideslips with the Douglas D-558-II (BuAero No. 37974) research airplane.

NASA Technical Library



3 1176 01436 3924